Research Article

Caiyun Zhang, Chunhong Li, Bolin Ji, and Zhaohui Jiang*

Preparation and application of carbon and hollow TiO_2 microspheres by microwave heating at a low temperature

https://doi.org/10.1515/epoly-2021-0014
received September 28, 2020; accepted December 17, 2020

Abstract: A fast, simple, and energy-saving microwave-assisted approach was successfully developed to prepare carbon microspheres. The carbon microspheres with a uniform particle size and good dispersity were prepared using glucose as the raw material and HCl as the dehydrating agent at low temperature (90°C) in an open system with the assistance of microwave heating. The carbon microspheres were characterized by elemental analysis, XRD, SEM, FTIR, TG, and Raman. The results showed that the carbon microspheres prepared under the condition of 18.5% (v/v) HCl and heating for 30 min by microwave had a narrow size distribution. The core–shell structure of the carbon core and TiO_2 shell was prepared with $(NH_4)_2TiF_6$, H_3BO_3 using the microwave-assisted method. The hollow TiO_2 microspheres with good crystallinity and high photocatalytic properties were successfully prepared by sacrificing the carbon microspheres.

Keywords: carbon microsphere, microwave-assisted method, normal atmosphere, low temperature, hollow TiO_2 microspheres

* **Corresponding author: Zhaohui Jiang,** Lutai School of Textile and Apparel, Shandong University of Technology, Shandong 255049, China, e-mail: jiangzhaohui@sdut.edu.cn
Caiyun Zhang: Lutai School of Textile and Apparel, Shandong University of Technology, Shandong 255049, China; College of Chemistry, Chemical Engineering and Biotechnology, Donghua University, Shanghai 201620, China
Chunhong Li: Lutai School of Textile and Apparel, Shandong University of Technology, Shandong 255049, China
Bolin Ji: College of Chemistry, Chemical Engineering and Biotechnology, Donghua University, Shanghai 201620, China

1 Introduction

The functionalized carbon microspheres with hydrophilic –OH and C═O groups have attracted great attention (1). These functional groups on the surface layer can bind metal cations through coordination or electrostatic interactions (2). Due to the abundant resource availability, nontoxic nature, environmental friendliness, and chemical stability, carbon microsphere has been widely used as energy storage (3–7), adsorbents (8–10), and catalyst supports (2,11,12). Simple monosaccharides, such as glucose (13), sucrose (14), etc., have been effectively employed as raw materials of carbon microspheres (15). However, the preparation of functionalized carbon microspheres has frequently been performed in harsh conditions. The preparation methods include hydrothermal method (16,17), chemical vapor deposition (18–20), template method (21–23), and pyrolysis technologies (21,24,25). The main barrier to the widespread use of carbon microsphere is the long duration and high reaction temperature required for the synthesis following the conventional methods (26). It makes the preparation costly and less competitive. It is reported that carbon microspheres can also be obtained by microwave-assisted hydrothermal method (3–5) with the advantages of saving time and competitive costs. However, as mentioned in literature, hydrothermal method was used in most cases of synthesis of carbon microspheres with microwave, which also requires a higher temperature (130–180°C) and high pressure (sealed reactor) (4). To our knowledge, carbon microspheres prepared by microwave-assisted method in open systems are less explored.

Titanium dioxide (TiO_2) was one of the most studied photocatalytic semiconductor materials due to its nontoxic, chemical stability, high catalytic activity, and low price in various semiconductor photocatalysts. Due to the unique properties of hollow microspheres such as good surface permeability, high refractive index, and large light-harvesting efficiencies (27), the preparation

of hollow TiO_2 microspheres has been receiving more and more attention.

In this study, carbon microspheres with good dispersity were prepared using glucose and HCl at 90°C by a fast and simple microwave-assisted method in an open system. Hollow TiO_2 microspheres were prepared by sacrificing the carbon microspheres. Then the photocatalytic performance of hollow TiO_2 was evaluated by the degradation of rhodamin B solution under the UV light irradiation.

2 Materials and methods

2.1 Materials

Glucose (analytical grade), hydrochloric acid (analytical grade), and boric acid (analytical grade) were provided by Sinopharm Chemical Reagent Co., Ltd. Ammonium hexafluorotitanate (analytical grade) was provided by Shanghai Shifan Chemical Co., Ltd. Rhodamin B (analytical grade) was provided by Shanghai Jingchun Reagent Co., Ltd. Degussa P25-TiO_2 was provided by Evonik Degussa Co., Ltd.

2.2 Synthesis of carbon microspheres

In a typical synthetic process, 4.0 g glucose in HCl solution was heated in a microwave reaction instrument (MAS-3-type universal microwave synthesis instrument; Xinyi Microwave Chemical Technology Co., Ltd., of input power 1,360 W) under normal pressure and 90°C. The product was separated by centrifugation and washed with deionized water for several times and dried at 80°C.

2.3 Synthesis of hollow TiO_2 microspheres

Carbon microspheres of 0.08 g were dispersed in deionized water with ultrasonic, and 0.6 mL of 0.50 mol/L H_3BO_3 aqueous solution was added. The mixture was heated at 90°C under microwave for 50 min. Then 0.3 mL of 0.50 mol/L $(NH_4)_2TiF_6$ aqueous solution was added to the mixture, which was heated at 90°C under microwave for further 60 min. After completion of reaction, the product was separated by centrifugation, washed with deionized water several times, and dried at 80°C. The product was calcined at 500°C for 1 h to get the hollow TiO_2 microspheres.

2.4 Photocatalytic decomposition of rhodamin B

The photocatalytic activity of the prepared TiO_2 and the commercial Degussa P25-TiO_2 (P25-TiO_2) was determined by measuring the photocatalytic degradation of rhodamin B (RhB). A 50 mL 5×10^{-5} mol/L RhB aqueous solution containing 0.03 g TiO_2 sample was radiated for different durations under 360 W UV lamp. The concentration of RhB was monitored by a UV-visible spectrophotometer.

2.5 Characterizations

The X-ray diffraction (XRD) was analyzed with a diffractometer (RIGAKU Max-2250PC X-ray diffractometer) employing Cu-Ka radiation. Surface morphology of the sample was observed using field-emission transmission electron microscope (FETEM; JEOL JEM-2100F). The functional groups of carbon microspheres were analyzed by using a US Nicolet/NEXUS-670 FTIR. The thermostability of carbon microspheres was tested using simultaneous thermal analyzer (TG, STA449F3). The elemental analysis of carbon microspheres was analyzed by using elemental analyzer (EA, Elmentar Vario EL III). The Raman spectrum was recorded on a Horiba Scientific LabRAM HR Evolution spectrometer.

3 Results

Carbon microspheres were synthesized by microwave-assisted carbonization in an open system, in which glucose and HCl were utilized as carbon source and dehydration catalyst, respectively. Then the TiO_2 shell was formed on the surface of the synthesized carbon microspheres under microwave radiation. Finally, the hollow TiO_2 microspheres with high photocatalytic properties were prepared by sacrificing carbon templates.

4 Discussion

The reaction conditions for carbon microspheres using HCl as dehydration catalyst are listed in Table 1. In the

condition of HCl and microwave-assisted heating, glucose molecules were dehydrated rapidly to form oligosaccharides and further hydrophobic polymers (1). The increasingly hydrophobic polymers further accelerated the phase separation and formed carbon microspheres by surface tension (28). Within the carbonaceous spherical polymer phase, the internal condensation reactions were also induced by the thermal and nonthermal effect of microwave and led to the final dehydration carbonization.

Table 1 shows the reaction temperature had a significant influence on the formation of carbon microspheres. It was found that no particles were formed in the solution below 90°C. It was proposed that the growth of carbon microspheres under microwave-assisted heating also followed LaMer model (29). When the temperature was below 90°C, the dehydration carbonization of glucose did not occur. As a result, the concentration of the aromatic compounds and oligosaccharide could not reach the critical concentration and the nucleation would not occur (30). The carbon microspheres could be only observed when the reaction temperature was above 90°C. However, this formation temperature was still lower than the reported temperature of hydrothermal formation of carbon microspheres (160–180°C) (31–33). The nonthermal effect of microwave irradiation should play a key influence on the formation of carbon microspheres at 90°C in an open system.

The elemental analysis (C, O, and H) of carbon microspheres in Table 1 shows that the carbon content (wt%) increases from ~36% in glucose to ~60% in carbon microspheres. It was noticed that the carbon content of samples A–C did not show significant change with increase in HCl concentration. For reaction time of 120 min, the carbon content of samples D–F showed a slight increase with an increase in HCl concentration. The results indicated that the influence of HCl concentration on the elementary composition was weaker than that of the reaction time. The reason was that the nonoxidative hydrochloride acid mainly acted as a dehydration catalyst during carbonization process, so the concentration of HCl didn't show a significant influence on the dehydration carbonization of glucose. It was found that all the samples of carbon microspheres contained less content of oxygen, which indicated the samples were partly carbonized. It was also noted in Table 1 that the H/C and O/C ratios of the carbon microspheres are much lower than those of glucose. According to the Van Krevelen diagram (34) (Figure 1), the evolution from glucose to carbon microspheres followed the diagonal line. This suggested that the decrease in H/C and O/C ratios of carbon microspheres was mainly caused by dehydration carbonization of glucose (34) under the hydrochloride acid and microwave irradiation.

The structure and composition of the products were investigated by XRD (Figure 2). The single broad peak in XRD at 2θ of ~23.0° corresponded to the (002) facet of carbon (partially graphitized) (35), which was characteristic of amorphous structure. This was consistent with the result of EA. The chemical structure of such partially carbonized materials could be described as –OH and –COOH substituted amorphous aromatic carbon (36). As compared with samples A, B, and D, the diffraction peaks of sample C, E, and F shifted to low degree, which indicated the space of graphite layer increased (37). As a result, the space of graphite layer of sample C, E, and F increased with the increase in the concentration of HCl and the reaction time.

The FETEM images in Figure 3 showed that the morphology of all products was almost spherical. However, the dispersity of samples A and D prepared under a low HCl condition was better when compared to other samples. Comparing the carbon microspheres prepared for

Table 1: Influence of reaction conditions on particle diameter and elemental analysis of carbon microspheres[a]

Sample	Reaction time (min)	HCl conc. (v/v)	Avg. particle diameter (nm)	Elemental analysis (wt%)			Atomic ratio	
				C	H	O	H/C	O/C
A	30	18.5%	340	60.04	4.37	35.59	0.87	0.44
B		25.9%	290	60.94	4.20	34.86	0.82	0.43
C		37.0%	280	60.38	4.18	35.44	0.83	0.44
D	120	18.5%	360	59.54	4.47	35.99	0.90	0.45
E		25.9%	310	63.28	4.32	32.40	0.82	0.38
F		37.0%	360	62.81	4.24	32.95	0.81	0.39
Glucose	—	—	—	36.36	7.07	56.57	2.33	1.17

[a] Reaction temperature was 90°C.

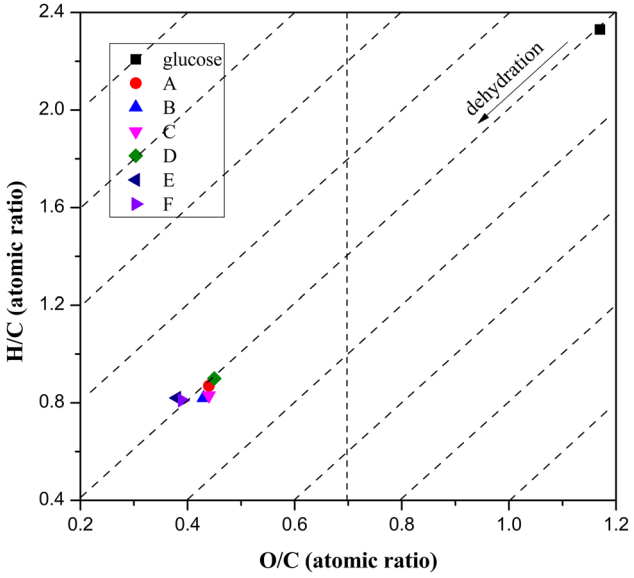

Figure 1: Van Krevelen diagram of glucose and carbon microspheres prepared under different conditions.

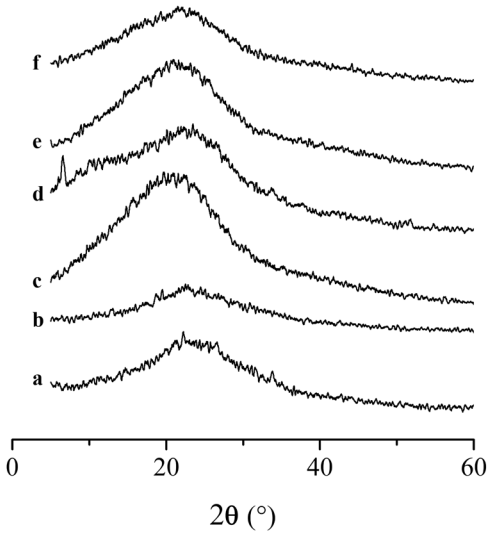

Figure 2: XRD of carbon microspheres prepared under different conditions. Samples (a–c) were prepared at 90°C for 30 min with different concentrations of HCl: (a) 18.5%, (b) 25.9%, (c) 37.0%. Samples (d–f) were prepared at 90°C for 120 min with different concentrations of HCl: (d) 18.5%, (e) 25.9%, (f) 37.0%.

30 min (Figure 3a–c) and 120 min (Figure 3d–f), it was obviously found that the heating time affected not only the diameter of carbon microspheres but also the aggregation of carbon microspheres. The possible reason was that the increasing system acidity accelerated the dehydration carbonization of glucose and further the polymerization reaction, which promoted the critical polymer concentration for nucleation. However, the polymer-rich condition also resulted in severe aggregation between carbon microspheres and broadened the size distribution. Sample A was chosen to detect the crystal form using FETEM testing because of its good spherical morphology. No lattice line was observed on the FETEM image (Figure 3a'), which indicated sample A was an amorphous structure. And the result was consistent with XRD.

FTIR spectra were used to identify the functional groups on the carbon microspheres (Figure 4). As compared with glucose, the spectra of carbon microspheres showed a significant change. The new band of carbon microspheres at ~1,640 cm^{-1} was attributed to the aromatic C=C vibrations (1), which indicated the aromatization of glucose during microwave-assisted heating. The presence of bands of carboxyl (–C=O) groups at ~1,700 cm^{-1} and –OH stretching vibration at ~3,400 cm^{-1} indicated that the reactive products with an abundance of hydroxyl functional groups, such as –COOH, were formed under the presence of hydrochloride acid and microwave irradiation. These hydroxyl functional groups further accelerated the condensation reactions and polymerization. The decrease in bands at 1,000–1,300 cm^{-1} assigned to the C–OH stretching and –OH bending in carbon microspheres (Figure 4a–f) also implied the condensation reactions and polymerization (38).

TG and DTG curves for glucose and carbon microspheres are shown in Figure 5. It was noticed that all the carbon microspheres showed similar TG curves, which indicated that the carbon content of carbon microspheres was almost the same. The difference in the TG curves between carbon microspheres and glucose revealed the dehydration of glucose under hydrochloric acid and microwave-assisted heating. Two weight loss stages were observed in the TG curves of carbon microspheres. The first weight loss that occurred at 95–110°C matched the moisture loss. The second stage of samples A–F was the main region of decomposition caused by the thermal decomposition of carbon microspheres. The extrapolated onset temperature of the second decomposition stage of samples A–F started at 241.8°C, 254.9°C, 280.5°C, 253.2°C, 281.8°C, and 287.1°C, respectively. And the correspond weight losses of the samples were 44.4%, 47.7%, 42.3%, 43.9%, 45.0%, and 43.6%. Little discrepancies were observed and it also suggested that the carbon contents in the samples were almost the same. All samples exhibited a single peak of slow thermal degradation. The temperature at maximum (T_{max}) degradation rate of samples A–F was 354.3°C, 380.6°C, 396.9°C, 354.6°C, 388.1°C, and 397.6°C, respectively. The TG curves showed that the carbon microspheres did not fully decompose even at 900°C, resulting in a consistent carbon residue. The initial

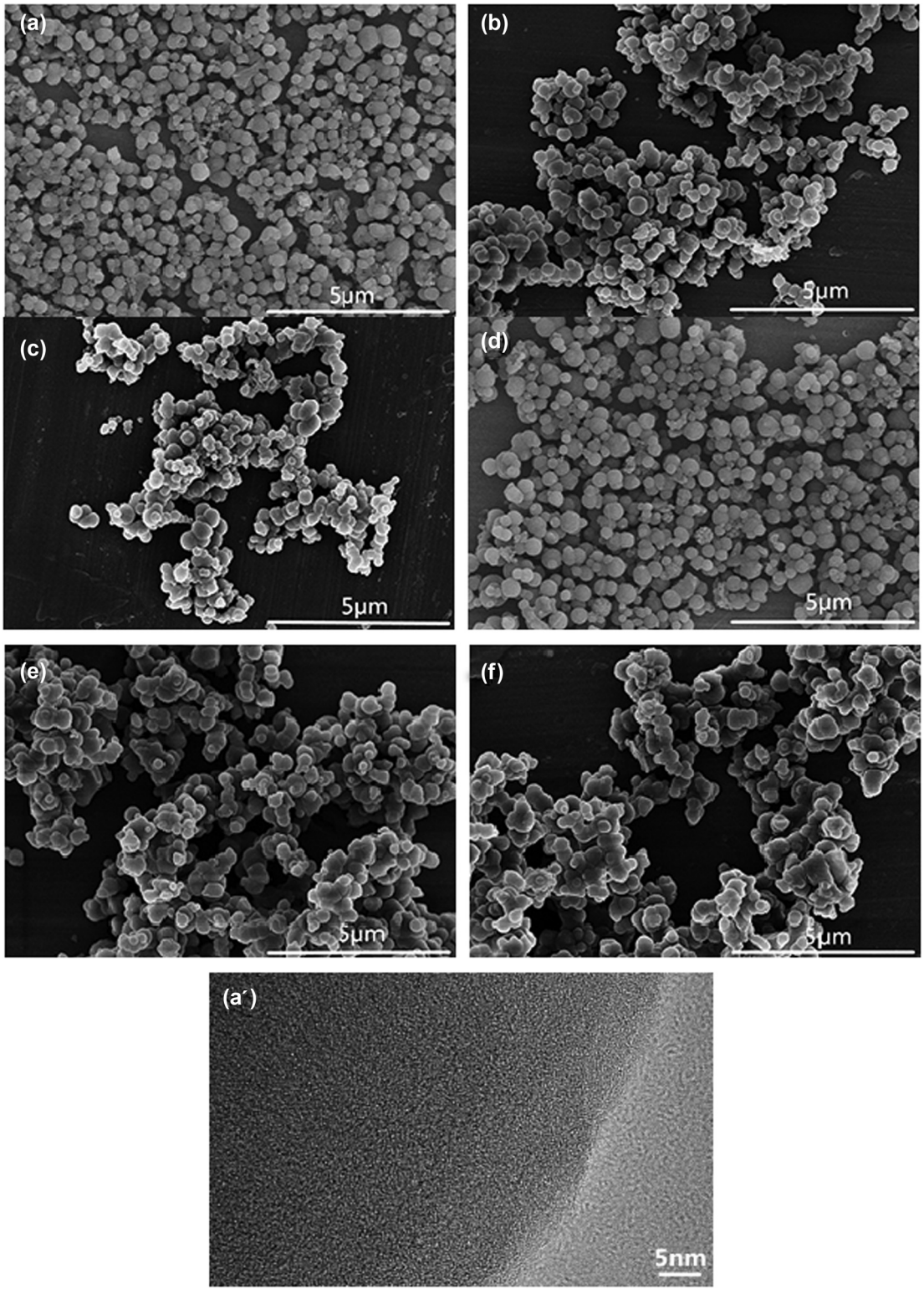

Figure 3: FESEM images of carbon microspheres prepared under different conditions and FETEM image of sample (a'). Samples (a–c) were prepared at 90°C for 30 min with different concentrations of HCl: (a) 18.5%, (b) 25.9%, (c) 37.0%. Samples (d–f) were prepared at 90°C for 120 min with different concentrations of HCl: (d) 18.5%, (e) 25.9%, (f) 37.0%.

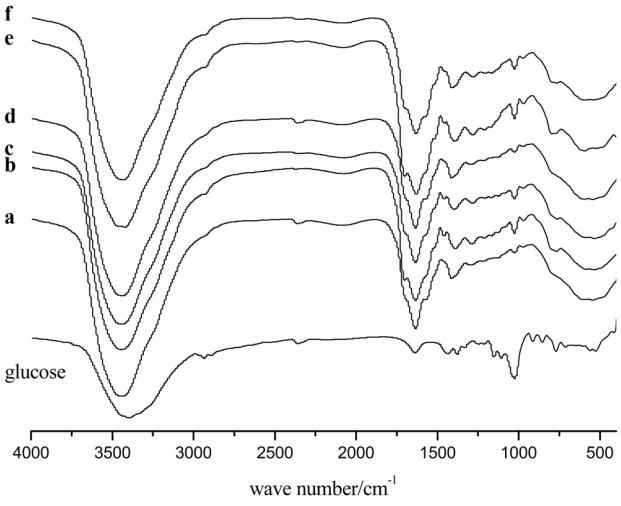

Figure 4: FTIR of glucose and carbon microspheres prepared under different conditions. Samples (a–c) were prepared at 90°C for 30 min with different concentrations of HCl: (a) 18.5%, (b) 25.9%, (c) 37.0%. Samples (d–f) were prepared at 90°C for 120 min with different concentrations of HCl: (d) 18.5%, (e) 25.9%, (f) 37.0%.

decomposition temperature of the second stage of samples A, B, and C (reaction time 30 min) and D, E, and F (reaction time 120 min) and the T_{max} increased with an increase in HCl concentration. This indicated the thermal stability and carbonization degree of carbon microspheres increased with an increase in HCl concentration. It could be found that in the carbon microspheres prepared under the same HCl concentration, i.e., A and D, B and E, and C and F, the thermal stability of the carbon microspheres increased with the increasing reaction time.

In the next experiment, the carbon microsphere (sample A) was selected as the template to prepare hollow TiO_2, and the structure of carbon microsphere (sample A) was characterized by Raman spectroscopy (Figure 6). The spectrum was characteristic of carbonized materials and two peaks appeared. The peak at approximately 1,380 cm^{-1} was assigned to the disordered graphite (D band) and the other at approximately 1,588 cm^{-1} corresponded to a splitting of the E_2^g stretching mode of graphite and reflected the structural intensity of the sp^2-hybridized carbon atom (G band) (39). This result was consistent with XRD.

The formation of TiO_2 shell on carbon microspheres was the key step for the formation of hollow TiO_2 microspheres. First, H_3BO_3 was adsorbed by carbon microspheres under microwave-assisted heating. Then the adsorbed H_3BO_3 molecules reacted with the added $(NH_4)_2TiF_6$ molecules on the surface of carbon microspheres. Due to the effective and unique heating mean of microwave, the formation and nucleation of TiO2 were both shorted. The hydrolysis reaction of $(NH_4)_2TiF_6$ in solution was as follows:

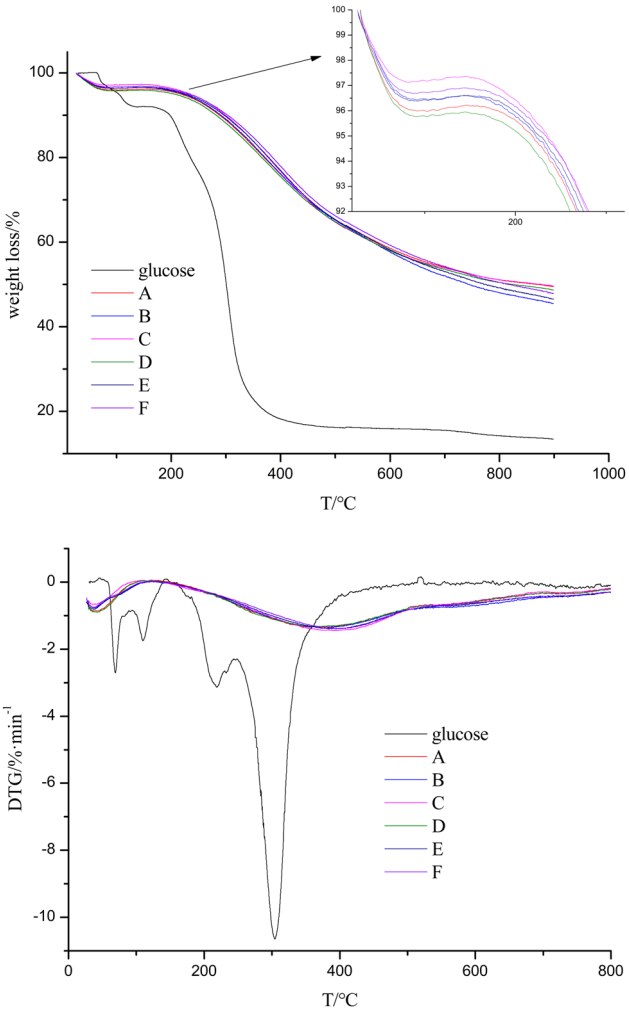

Figure 5: TG and DTG curves of glucose and carbon microspheres prepared under different conditions.

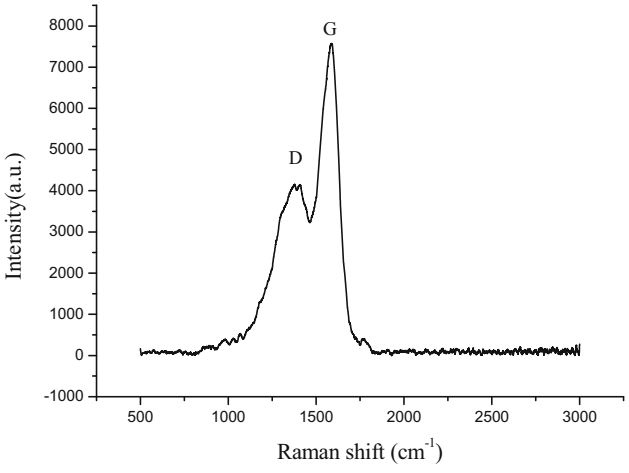

Figure 6: Raman spectrum of sample A.

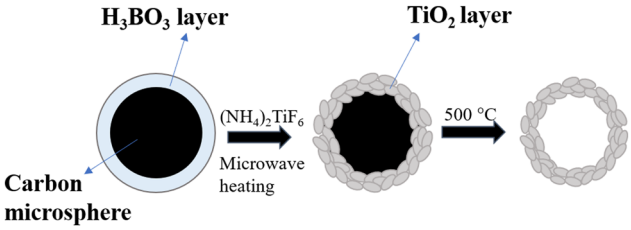

Figure 7: Schematic diagram of preparing hollow TiO_2.

$$[TiF_6]^{2-} + nH_2O \rightarrow [TiF_{6-n}(OH)_n]^{2-} + nHF$$
$$H_3BO_3 + 4HF \rightarrow BF_4^- + H^+ + 3H_2O$$
$$[Ti(OH)_6]^{2-} + 2H^+ \rightarrow TiO_2 + 4H_2O$$

The schematic diagram was shown in Figure 7.

Figure 8 showed the sharp peaks corresponded to the anatase phase of TiO_2 (JCPDS No. 21-1272, space group *I*41/*amd* (141)), and the broad peak in Figure 8a and b at 2θ of ~23.0° corresponded to the (002) facet of carbon (40). This indicated that anatase TiO_2 was loaded on the carbon microspheres. All peaks in XRD (Figure 8c) of the calcined TiO_2–C could be indexed as anatase phase of TiO_2. The broad peak of carbon microspheres at ~23.0° disappeared after calcination. This indicated that the pure anatase TiO_2 was obtained after calcination. The pure TiO_2 was also synthesized by the mentioned microwave-assisted method and characterized by XRD (Figure 8d). The result also indicated the formation of typical anatase TiO_2.

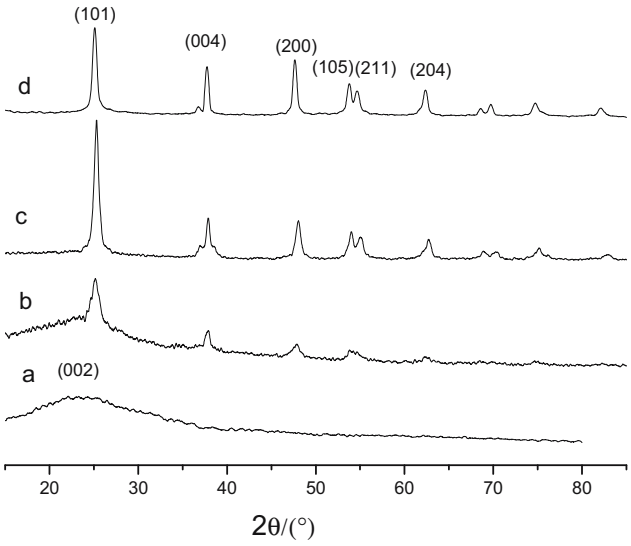

Figure 8: XRD of different samples: (a) carbon microspheres; (b) TiO_2–C; (c) the calcined TiO_2–C; (d) TiO_2.

FESEM image of the core–shell (TiO_2–C) structure and the calcined TiO_2–C is shown in Figure 9, and the TiO_2–C core–shell structure (Figure 9a) had a regular ball shape with a rough surface and relatively uniform particle size (about 590 nm). The overall morphology of the calcined TiO_2–C is shown in Figure 9b. A few broken microspheres with dark contrast in the center region was observed, indicating their hollow structures. The hollow structure was

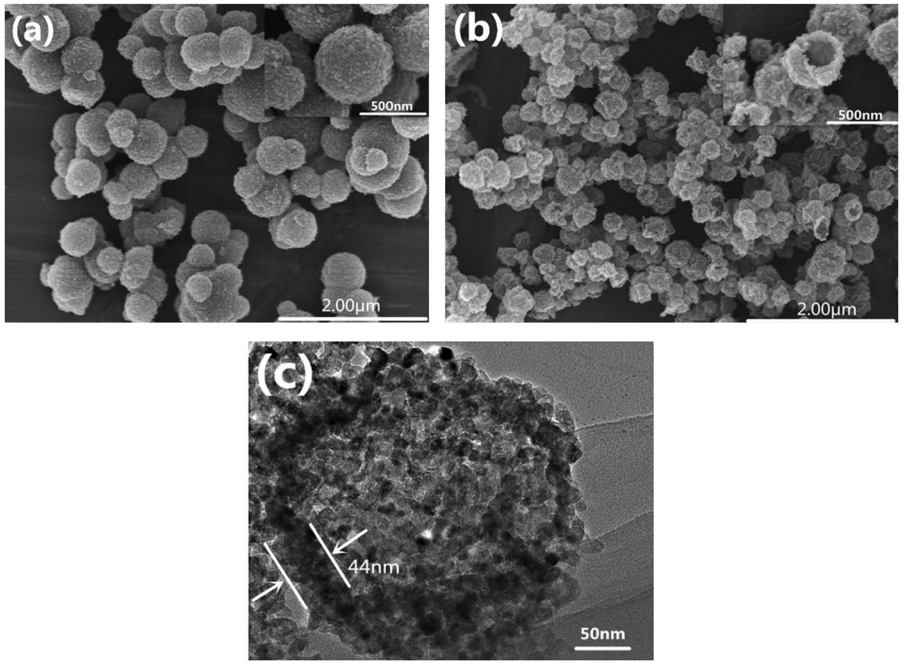

Figure 9: FESEM images of TiO_2–C and hollow TiO_2 microspheres and FETEM images of hollow TiO_2 microspheres: (a) TiO_2–C; (b and c) hollow TiO_2 microspheres.

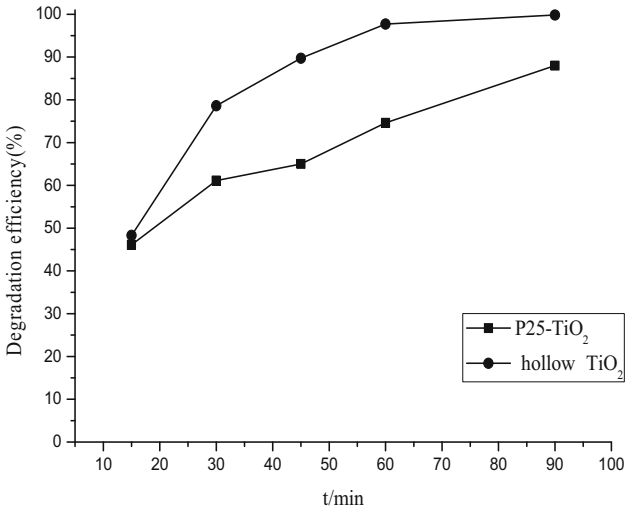

Figure 10: Photocatalytic activity of prepared hollow TiO_2 microspheres and P25-TiO_2.

further evidenced by FETEM (Figure 9c). Figure 9c was a magnified view of a representative hollow microsphere. It could be seen (Figure 9c) that the microsphere was hollow and nanoporous and formed by colloidal aggregation, consistent with Figure 9b. The diameters of hollow TiO_2 microspheres were about 263 nm with a thickness of about 44 nm (Figure 9c).

The photocatalytic activity of P25-TiO_2 and the prepared hollow TiO_2 microspheres were evaluated by the UV photocatalytic degradation of RhB aqueous solution at the ambient temperature. Figure 10 shows the degradation ratio of RhB. It could be seen that the hollow TiO_2 microspheres had a high photocatalytic activity. After 30 min of catalysis by hollow TiO_2 microspheres under UV irradiation, the photocatalytic degradation rate of RhB reached 85% higher than that of P25-TiO_2 (71%). After 60 min, the photocatalytic degradation rate reached 96% (P25-TiO_2 78%). This indicated that the hollow TiO_2 microspheres had high photocatalytic properties. It had been suggested that hollow spherical microstructures with hierarchical shell walls

could be beneficial to increase light harvesting (41) or increased the photocatalytic activity by solvent entrapment and sequestration (42).

5 Conclusions

The synthesis strategy utilized in this study made it possible to rapidly synthesize the carbon microspheres at low temperature (90°C) in an open system by microwave-assisted method. The carbon microspheres with uniform particle size and good dispersity were prepared using glucose as raw materials under low HCl concentration (18.5%). The HCl concentration and microwave heating time did not show significant influence on the elemental composition, thermal stability, and carbonization degree of carbon microspheres. By using carbon microspheres as template, the hollow TiO_2 microspheres were successfully prepared with $(NH_4)_2TiF_6$ and H_3BO_3 as raw materials. This simple method provided an efficient and easy-controlling method to synthesize carbon microspheres and the hollow TiO_2 microspheres from environmentally friendly materials under mild reaction condition. Moreover, the hollow TiO_2 microspheres had high photocatalytic properties.

Research funding: Authors state no funding involved.

Author contribution: The manuscript was written through contributions of all authors. All authors have given approval to the final version of the manuscript.

Conflict of interest: Authors state no conflict of interest.

References

(1) Sun X, Li Y. Colloidal carbon spheres and their core/shell structures with noble-metal nanoparticles. Angew Chem Int Ed. 2004;43(5):597–601. doi: 10.1002/anie.200352386.
(2) Hu Y, Liu Y, Qian H, Li Z, Chen J. Coating colloidal carbon spheres with CdS nanoparticles: microwave assisted synthesis and enhanced photocatalytic activity. Langmuir. 2010;26(23):18570–5. doi: 10.1021/la103191y.
(3) Jung A, Han S, Kim T, Cho WJ, Lee KH. Synthesis of high carbon content microspheres using 2-step microwave carbonization, and the influence of nitrogen doping on catalytic activity. Carbon. 2013;60:307–16. doi: 10.1016/j.carbon.2013.04.042.
(4) Chen T, Pan L, Lu T, Fu C, Chua D, Sun Z. Fast synthesis of carbon microspheres via a microwave-assisted reaction for sodium ion batteries. J Mater Chem A. 2013;2:1263–7. doi: 10.1039/c3ta14037g.
(5) Sun H, Chen T, Liu Y, Hou X, Zhang L, Zhu G, et al. Carbon microspheres via microwave-assisted synthesis as counter electrodes of dye-sensitized solar cells. J Colloid Interf Sci. 2015;445:326–9. doi: 10.1016/j.jcis.2015.01.016.
(6) He Y, Cheng Z, Zuo H, Yan C, Liao Y. Green synthesis of pyridyl conjugated microporous polymers as precursors for porous carbon microspheres for efficient electrochemical energy storage. Chem Electro Chem. 2020;7(4):959–66. doi: 10.1002/celc.201901975.
(7) Diez N, Sevilla M, Fuertes AB. Highly-packed monodisperse porous carbon microspheres for energy storage in

supercapacitors and Li–S batteries. Chem Electro Chem. 2020;18(7):3798–810. doi: 10.1002/celc.202000960.
(8) Chen LF, Liang HW, Lu Y, Cui CH, Yu SH. Synthesis of an attapulgite clay@carbon nanocomposite adsorbent by a hydrothermal carbonization process and their application in the removal of toxic metal ions from water. Langmuir. 2011;27(14):8998–9004. doi: 10.1021/la2017165.
(9) Yang W, Xu G, Shu J, Wang M, Ge X. Preparation and adsorption property of novel inverse-opal hierarchical porous N-doped carbon microspheres. Chin Chem Lett. 2020 (in press). doi: 10.1016/j.cclet.2020.06.004.
(10) Ma J, Sun M, Zeng Y, Liu Z, Zhang M, Xiao Y, et al. Acetylacetone functionalized magnetic carbon microspheres for the highly-efficient adsorption of heavy metal ions from aqueous solutions. RSC Adv. 2019;9(6):3337–44. doi: 10.1039/C8RA09830A.
(11) Auer E, Freund A, Pietsch J, Tacke T. Carbons as supports for industrial precious metal catalysts. Appl Catal A Gen. 2010;30(2):259–71. doi: 10.1002/chin.199906260.
(12) Guo T, Qin X, Hou L, Li J, Li X, Liang Q. Waxberry-like hierarchical $NiCo_2O_4$-decorated carbon microspheres as efficient catalyst for Li-O_2 batteries. J Solid State Electr. 2019;23:1359–69. doi: 10.1007/s10008-019-04222-8.
(13) Qi X, Lian Y, Yan L, Smith RL. One-step preparation of carbonaceous solid acid catalysts by hydrothermal carbonization of glucose for cellulose hydrolysis. Acta Chim Sin. 2014;57:50–4. doi: 10.1016/j.catcom.2014.07.035.
(14) Sevilla M, Fuertes AB. Chemical and structural properties of carbonaceous products obtained by hydrothermal carbonization of saccharides. Chem Eur J. 2009;15:4195–203. doi: 10.1002/chem.200802097.
(15) Titirici MM, Antonietti M, Baccile N. Hydrothermal carbon from biomass: a comparison of the local structure from poly-to monosaccharides and pentoses/hexoses. Green Chem. 2008;10(11):1204–12. doi: 10.1039/b807009a.
(16) Chen X, Lai Y, Gu Y, Jiao C, Li S. Effect of functionalized carbon microspheres combined with ammonium polyphosphate on fire safety performance of thermoplastic polyurethane. ACS Omega. 2020;5(11):6051–61. doi: 10.1021/acsomega.9b04462.
(17) Khan TA, Kim HJ, Gupta A, Jamari SS, Jose R. Synthesis and characterization of carbon microspheres from rubber wood by hydrothermal carbonization. J Chem Technol Biot. 2019;94(5):1374–83. doi: 10.1002/jctb.5867.
(18) Wu HC, Hong CT, Chiu HT, Li YY. Continuous synthesis of carbon spheres by a non-catalyst vertical chemical vapor deposition. Diam Relat Mater. 2009;18(4):601–5. doi: 10.1016/j.diamond.2008.10.047.
(19) Jin YZ, Gao C, Hsu WK, Zhu Y, Huczko A, Bystrzejewski M, et al. Large-scale synthesis and characterization of carbon microspheres prepared by direct pyrolysis of hydrocarbons. Carbon. 2005;43(9):1944–53. doi: 10.1016/j.carbon.2005.03.002.
(20) Wu F, Wang C, Hu HY, Pan M, Dai GP. Controlled synthesis of N-doped carbon microspheres from melamine-based carbon by chemical vapor deposition. Chem Phys Lett. 2019;730:124–9. doi: 10.1016/j.cplett.2019.05.041.
(21) Pol VG, Motiei M, Gedanken A, Calderon-Moreno J, Yoshimura M. Carbon spherules: synthesis, properties and mechanistic elucidation. Carbon. 2004;42(1):111–6. doi: 10.1016/j.carbon.2003.10.005.
(22) Li F, Huang J, Zou J, Pan P, Yuan G. Preparation and characterization of porous carbon beads and their application in dispersing small metal crystallites. Carbon. 2002;40(15):2871–7. doi: 10.1016/S0008-6223(02)00224-5.
(23) Xu W, Song W, Liu F, Wang Z, Jin G, Li C, et al. Facile synthesis of N-doped hollow carbon spheres @MoS_2 via polymer microspheres template method and one-step calcination for enhanced hydrogen evolution reaction. Chem Electro Chem. 2019;6(4):1101–6. doi: 10.1002/celc.201801469.
(24) Park GD, Kang YC, Yoo Y. Carbon microspheres with micro- and mesopores synthesized via spray pyrolysis for high-energy-density, electrical-double-layer capacitors. Chem Eng J. 2019;365:193–200. doi: 10.1016/j.cej.2019.02.036.
(25) Anceschi A, Binello A, Caldera F, Trotta F, Zanetti M. Preparation of microspheres and monolithic microporous carbons from the pyrolysis of template-free hyper-crosslinked oligosaccharides polymer. Molecules. 2020;25(13):3034. doi: 10.3390/molecules25133034.
(26) Hu Y, Zhou Y, Wang J, Shao Z. Preparation and characterization of macroporous LiNi1/3Co1/3Mn1/3O2 using carbon sphere as template. Mater Chem Phys. 2011;129(1–2):296–300. doi: 10.1016/j.matchemphys.2011.04.007.
(27) Ao Y, Xu J, Fu D, Yuan C. Visible-light responsive C,N-codoped Titania hollow spheres for X-3B dye photodegradation. Microporous Mesoporous Mater. 2009;118(1–3):382–6. doi: 10.1016/j.micromeso.2008.09.010.
(28) Li H, He X, Liu Y, Huang H, Lian S, Lee ST, et al. One-step ultrasonic synthesis of water-soluble carbon nanoparticles with excellent photoluminescent properties. Carbon. 2011;49(2):605–9. doi: 10.1016/j.carbon.2010.10.004.
(29) Huang Y, Pemberton JE. Synthesis of uniform, spherical sub-100 nm silica particles using a conceptual modification of the classic LaMer model. Colloid Surf A. 2010;360(1–3):175–83. doi: 10.1016/j.colsurfa.2010.02.031.
(30) Lee KU, Park KJ, Kwon OJ, Kim JJ. Carbon sphere as a black pigment for an electronic paper. Curr Appl Phys. 2013;13(2):419–24. doi: 10.1016/j.cap.2012.09.003.
(31) Rolland JP, Hagberg EC, Denison GM, Carter KR, Simone JMD. High-resolution soft lithography: enabling materials for nanotechnologies. Angew Chem Int Ed. 2010;43(43):5796–9. doi: 10.1002/anie.200461122.
(32) Yao C, Shin Y, Wang LQ, Windisch CF, Samuels WD, et al. Hydrothermal dehydration of aqueous fruc. J Phys Chem C. 2007;111(42):15141–5. doi: 10.1021/jp074188l.
(33) Luijkx GCA, Rantwijk FV, Bekkum HV, Antal MJ. The role of deoxyhexonic acids in the hydrothermal decarboxylation of carbohydrates. Carbohydr Res. 1995;272(2):191–202. doi: 10.1016/0008-6215(95)00098-E.
(34) Guiotoku M, Rambo C, Maia C, Hotza D. Synthesis of carbon-based materials by microwave hydrothermal processing. Usha Chandra, London: IntechOpen Limited; 2011.
(35) Hu ZF, Yan ZX, Shen PK, Zhong CJ. Nano-architectures of ordered hollow carbon spheres filled with carbon webs by template-free controllable synthesis. Nanotechnology. 2012;23(48):485404–14. doi: 10.1088/0957-4484/23/48/485404.

(36) Titirici MM, Thomas A, Yu SH, Müller JO, Antonietti M. A direct synthesis of meosporous carbons with bicontinuouspore morphology from crude plant material by hydrothermal carbonization. Chem Mater. 2007;19(17):4205–12. doi: 10.1021/cm0707408.
(37) Zheng MT, Xiao Y, Zhang HR, Dong HW, Liu XT. Hydrothermal synthesis and characterization of sulfur-doped carbon microspheres. Chin J Inorg Chem. 2013;29(7):1391–9. doi: 10.3969/j.issn.1001-4861.2013.00.244.
(38) Krevelen DWV. Graphical-statistical method for the study of structure and reaction processes of coal. Fuel. 1950;29:269–84.
(39) Schuepfer DB, Badaczewski F, Guerra-Castro JM, Hofmann DM, Klar PJ. Assessing the structural properties of graphitic and non-graphitic carbons by Raman spectroscopy. Carbon. 2020;161:359–72. doi: 10.1016/j.carbon.2019.12.094.
(40) Hu ZF, Yan Z, Shen PK, Zhong CJ. Nano-architectures of ordered hollow carbon spheres filled with carbon webs by template-free controllable synthesis. Nanotechnol. 2012;23:485404–14. doi: 10.1088/0957-4484/23/48/485404.
(41) Yu J, Zhang L, Cheng B, Su Y. Hydrothermal preparation and photocatalytic activity of hierarchically sponge-like macro-/mesoporous titania. J Phys Chem C. 2007;111(28):10582–9. doi: 10.1021/jp0707889.
(42) Yu J, Yu H, Guo H, Li M, Mann S. Spontaneous formation of a tungsten trioxide sphere-in-shell superstructure by chemically induced self-transformation. Small. 2008;4(1):87–91. doi: 10.1002/smll.200700738.